Stem Cell Reports, Volume *12*

Supplemental Information

Clonal and Quantitative *In Vivo* Assessment of Hematopoietic Stem Cell Differentiation Reveals Strong Erythroid Potential of Multipotent Cells

Scott W. Boyer, Smrithi Rajendiran, Anna E. Beaudin, Stephanie Smith-Berdan, Praveen K. Muthuswamy, Jessica Perez-Cunningham, Eric W. Martin, Christa Cheung, Herman Tsang, Mark Landon, and E. Camilla Forsberg

SUPPLEMENTAL TABLE 1

	RBC	Plt	GM	B	T
HSC	51.2	16.1	31.2	0.91	0.27
MPP^F	96.1	0.73	2.30	0.56	0.28
CMP	99.7	0.20	0.07	nd	nd
CMP^F	98.8	0.37	0.85	nd	nd
GMP	87.2	0.68	12.1	nd	nd
MEP	99.9	0.13	nd	nd	nd
CLP	nd	nd	nd	92.4	7.6

Supplemental Table 1: Proportion of each mature cell type generated from each progenitor cell population during the entire 110 day time course of the transplantation experiments in Figure 1 calculated using an “extreme half-life” scenario (illustrated in Figure S3).

SUPPLEMENTAL TABLE 2

	Total numbers of cells	
Cell type	Burst phase method	Extreme half-life method
HSC	6,502,000	48,496,584
MPP^F	803,400	1,035,218
CMP	140,380	188,077
CMP^F	35,210	45,467
GMP	47	54
MEP	32,029	39,002
CLP	462	1,189

Supplemental Table 2: The estimated numbers of total cells produced per transplanted stem/progenitor cell are similar whether derived by the “burst phase” method or by the “extreme half-life” method (illustrated in Figure S3). The “burst phase method” was used as in Figure 2 and Table 1 of the manuscript and the “extreme half-life” method in Figure S2A’-G’, and Table S1. Because progenitors only produce significant numbers of new cells during the burst phase, the two methods largely agree. This is not true for HSCs, as they self-renew and give rise to an indefinite number of cells.

Supplemental Figure 1

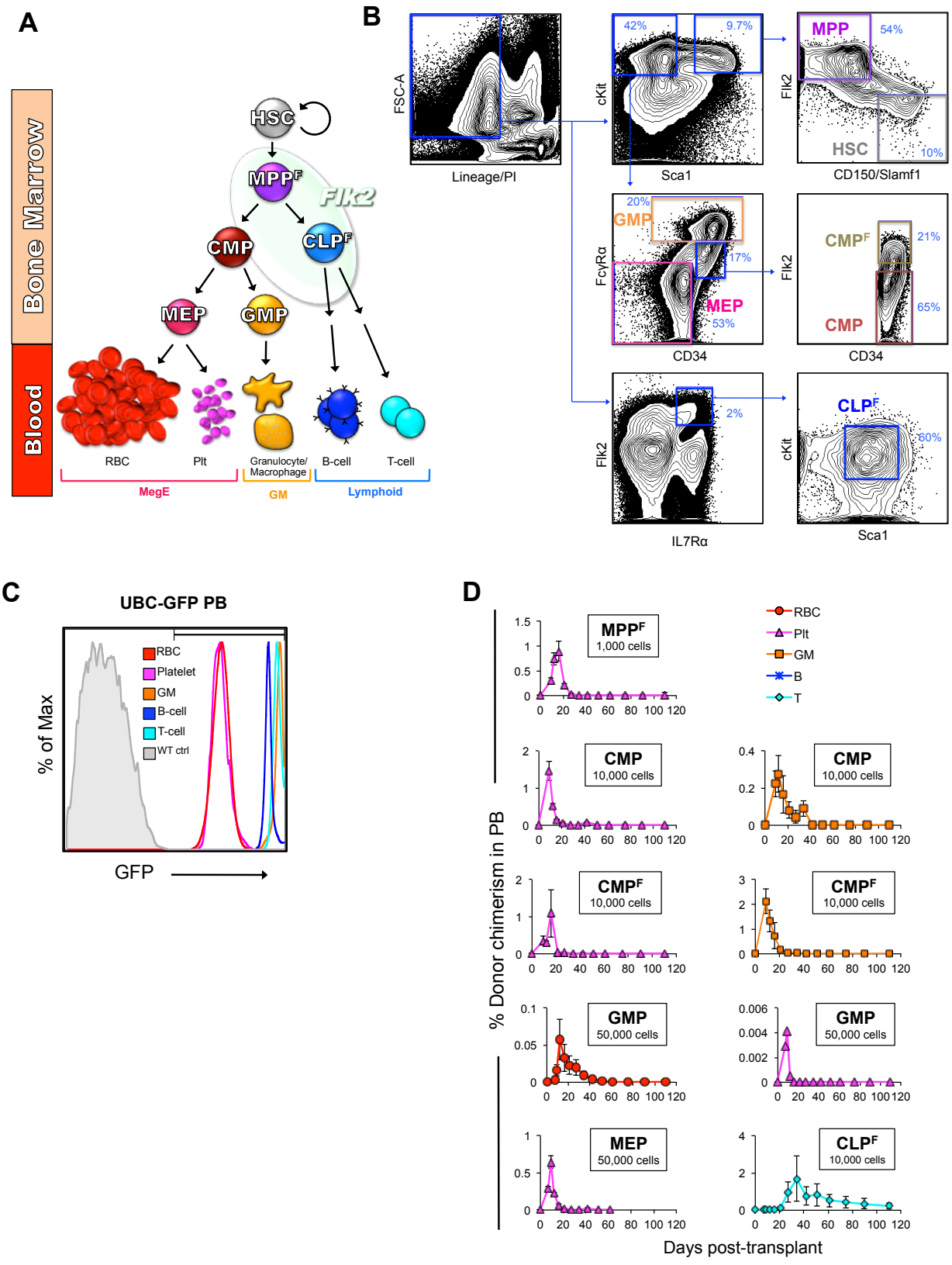

Supplemental Figure 1: Transplantation strategy for evaluating lineage potentials from various HPSCs double-sorted from UBC-GFP mice.

(**A**) Schematic of hematopoietic differentiation to illustrate the terminology used for cell types and lineages in the text.

(**B**) FACS-sorting strategy for isolating hematopoietic subtypes. Cells were pre-gated for singlets only (FSC-W^{low}). Bone marrow was cKit-enriched prior to FACS-sorting of transplanted cell types, with the exception of CLPs where lineage-depletion was used instead of cKit enrichment.

(**C**) Flow cytometry analysis of peripheral blood (PB) cells from UBC-GFP mice showing high levels of GFP expression in both nucleated and enucleated hematopoietic cell types.

(**D**) Reconstitution data from Figure 1B-G, replotted as separate, mature donor-derived cells on different y-axis scales to visualize lineages with low levels of donor chimerism.

HSC – Hematopoietic Stem Cell; MPP^F – Multipotent Progenitor; CMP – Common Myeloid Progenitor; CMP^F – FLK2+ Common Myeloid Progenitor; CLP^F – Common Lymphoid Progenitor; GMP – Granulocyte/Myelomonocyte Progenitor; MEP – Megakaryocyte/Erythrocyte Progenitor; RBC - Red Blood Cell; Plt - Platelet; GM - Granulocyte/Myelomonocyte.

Supplemental Figure 2

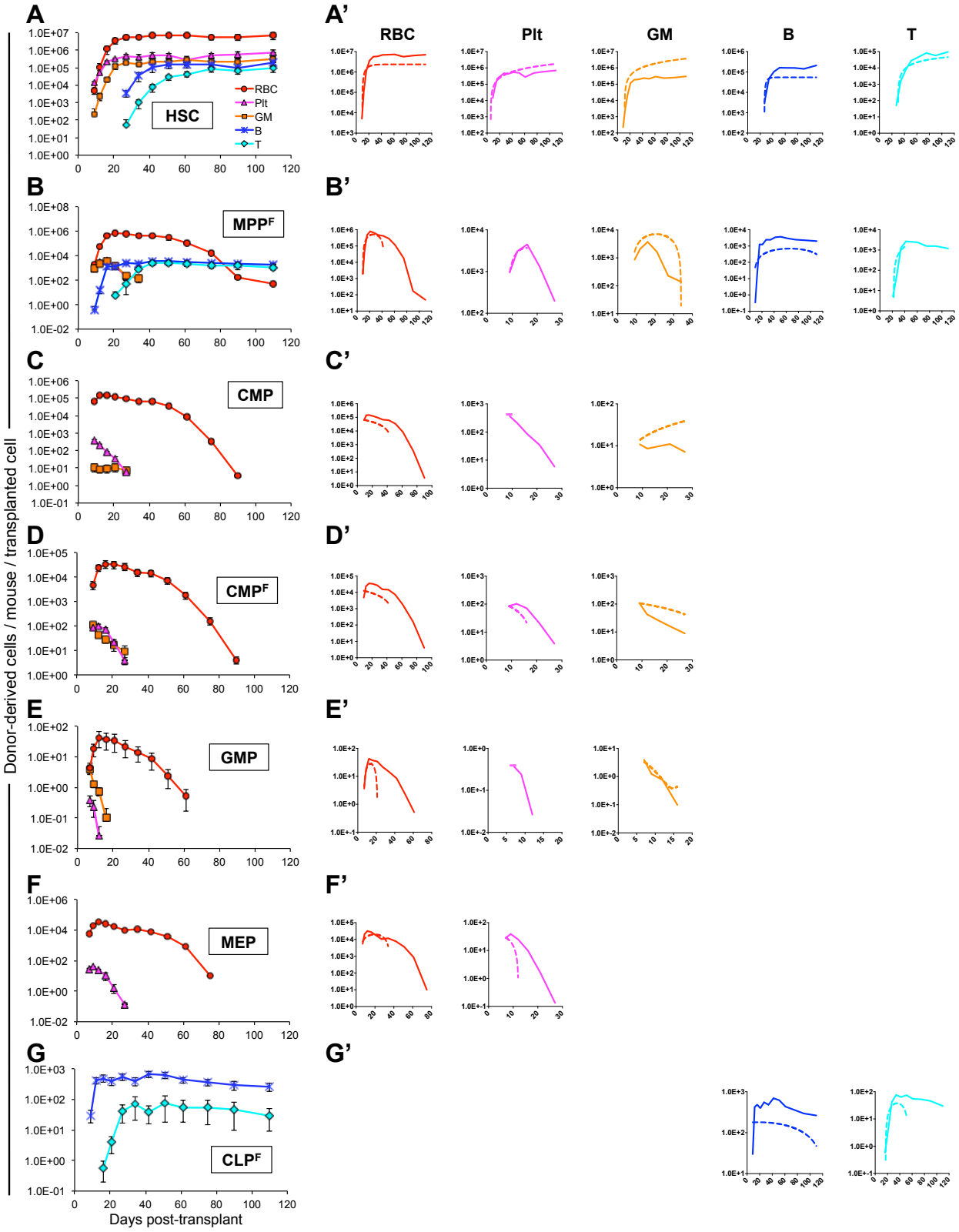

Supplemental Figure 2: Total numbers of mature cells generated per transplanted cell. (**A-G**) Absolute number of donor-derived mature cells present in a mouse over time post-transplantation per transplanted donor cell. Enumeration of donor-derived mature cells in **Figure 1M-S** was used in combination with total mature cell number in the PB (**Figure 1I**) and mature cell distribution (**Figure 1J**) to estimate the total number of mature cells in the entire recipient derived from each HSPC after transplantation.

(**A'-G'**) Calculated absolute number of donor-derived mature cells generated in a mouse over time post-transplantation per transplanted donor cell based on an "extreme half-life" Markov Modeling approach. The numbers in panels A-G were used to estimate new mature cells generated by accounting for the differential half-life, and therefore different extents of cell accumulation, of the different mature cell types. The individual plots for RBCs, Plts, GM, B and T cells provide a side-by-side comparison of "cells present" (solid lines, from the A-G data in the left column) versus "new cells produced" (dashed lines; from the Markov-transformed data) by each transplanted HSC or progenitor cell, as indicated. The solid lines end when the number of donor-derived cells in the peripheral blood approaches zero (or for HSCs, when the experiment was ended). The dashed lines end when new cell production ceased. Note that cells with a shorter half-life (such as GMs) are newly produced at a higher rate than apparent from the "cells present" data (dashed lines are above solid lines), whereas cells with longer half-lives (such as RBCs) accumulate (solid lines are above dashed lines).

Supplemental Figure 3

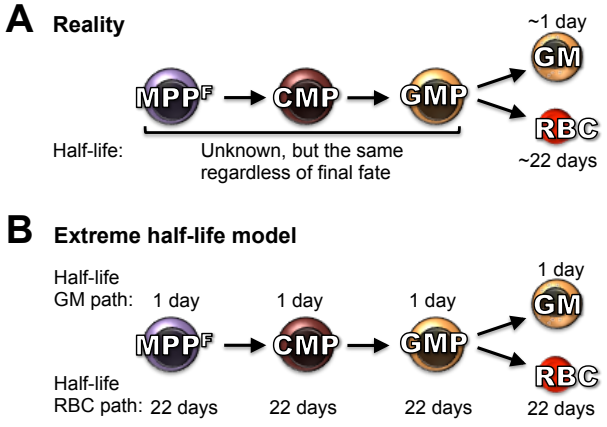

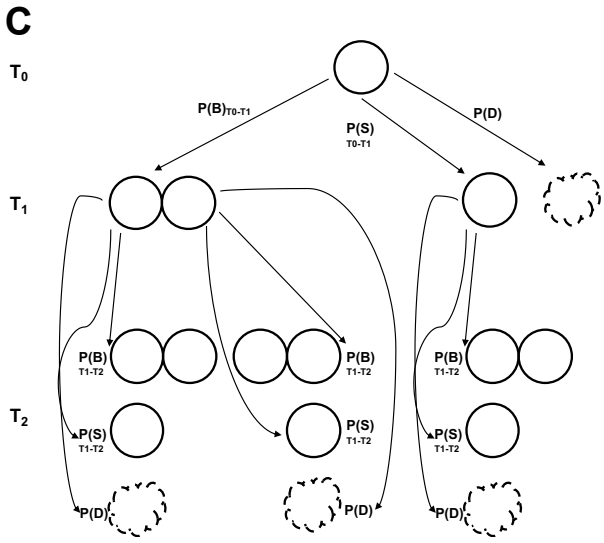

Supplemental Figure 3: Cartoon to illustrate the "extreme half-life" scenario.

(**A**) We know that the approximate half-lives of mature hematopoietic cells vary many fold, but we do not know the half-life of progenitor populations. We also do not know the exact path of differentiation; a hypothetical example of MPPs giving rise to GMs and RBCs via CMPs and GMPs is given to illustrate the concept. In Markov-based calculations to estimate "new mature cells produced", we used the "extreme half-life" scenario (**B**) where we assigned all progenitors of RBCs a 22-day half-life, and all the progenitors of GMs a 1-day half-life, etc. This exaggerates the differences between the "new" and "accumulated" cells, yet the proportions (Table S1) and total numbers (Table S2) of cells produced/accumulated by each progenitor cell lead to very similar conclusions.

(**C**) Schematic of probabilities in the Modified Markov birth/death model. $P(B)_t$, time-dependent probability of birth; P(D), probability of death (calculated based on published half-lives for each mature cell type); $P(S)_t$ probability of no change ($P(S)_t = 1-P(B)_t -P(D)$).

Supplemental Figure 4

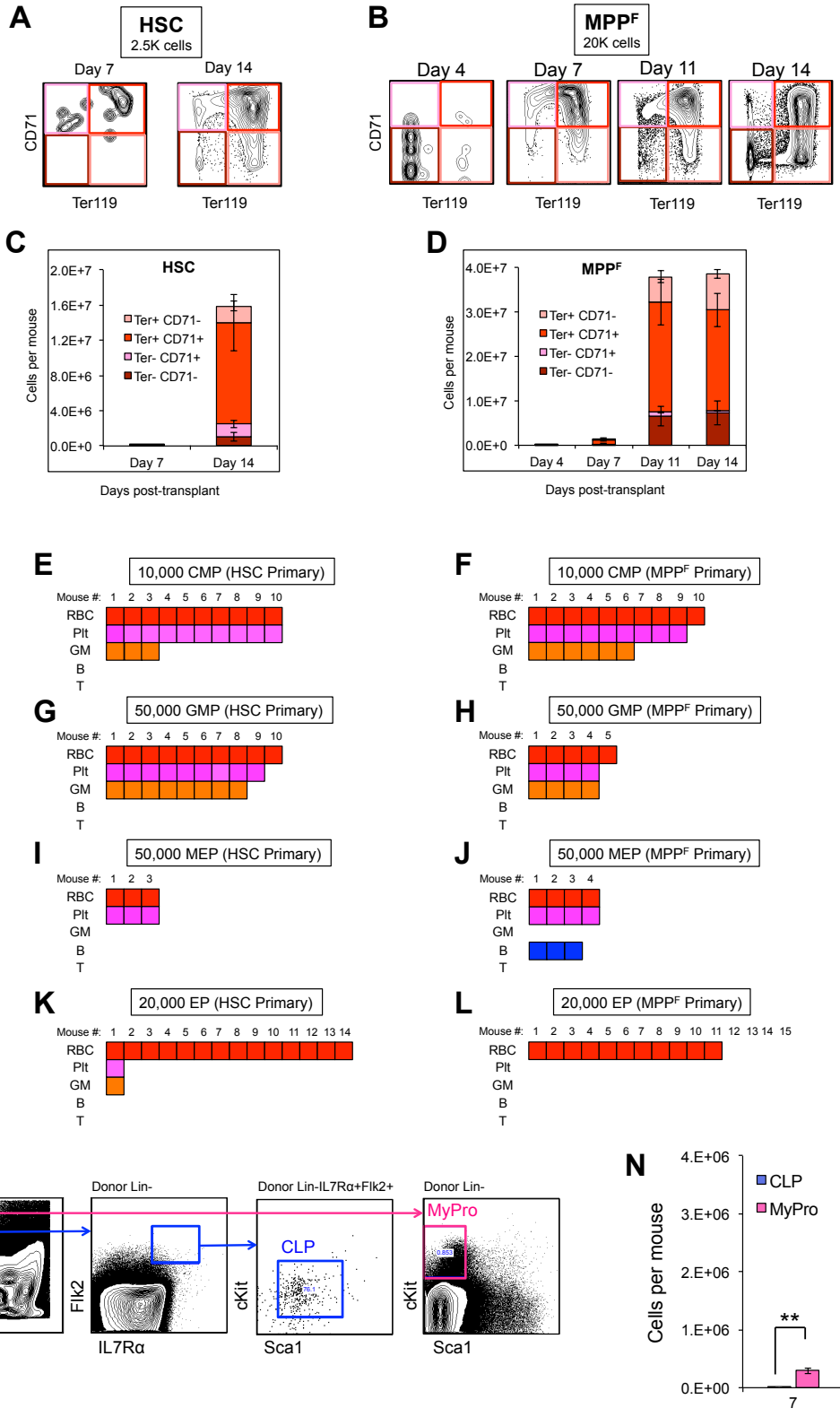

Supplemental Figure 4: Quantification and functional assessment of HSC- and MPP^F-derived progenitor cells.

(**A-B**) Sub-fractionation of donor-derived $Gr1^-Mac1^-B220^-CD3^-$ cells displayed in Figure 4 H^1-$I^{4'}$ by CD71 and TER-119. HSCs and MPP^Fs give rise to all four populations, and the proportions of cells generated by HSCs and MPP^F are similar. Analyses were performed after 4, 7, 11 and 14 days of 2,500 HSCs (A) or 20,000 MPP^Fs (B) transplantation into lethally irradiated hosts.

(**C-D**) Quantification of results displayed in A-B. n=4 to 9 recipients in at least 2 independent experiments (HSC and MPP^F).

(**E-L**) Functional testing by secondary transplantation of progenitor cells produced by HSCs and MPP^Fs in Figure 4 show that these phenotypic progenitor cells have similar functional properties as in primary transplantation. Mature cell detection by flow cytometry is indicated for each recipient and cell type by a filled square (RBCs, red; Plts, pink; GMs, orange; B cells, blue; T cells, teal). Three independent experiments are shown with the number of individual recipients indicated for each transplanted cell type.

(**M-N**) Transplanted MPP^F give rise to higher numbers of myeloid than lymphoid progenitors shortly after transplantation. MPP^F (20,000 cells per recipient) were transplanted into lethally irradiated recipients, followed by analysis of myeloid and lymphoid progenitors in the BM at 7 and 14 days after transplantation. n=4-6 recipients in 3 independent experiments for each analysis timepoint. Data are displayed as means ± SEM. ** $P<0.005$, *** $P<0.001$.

Supplemental Figure 5

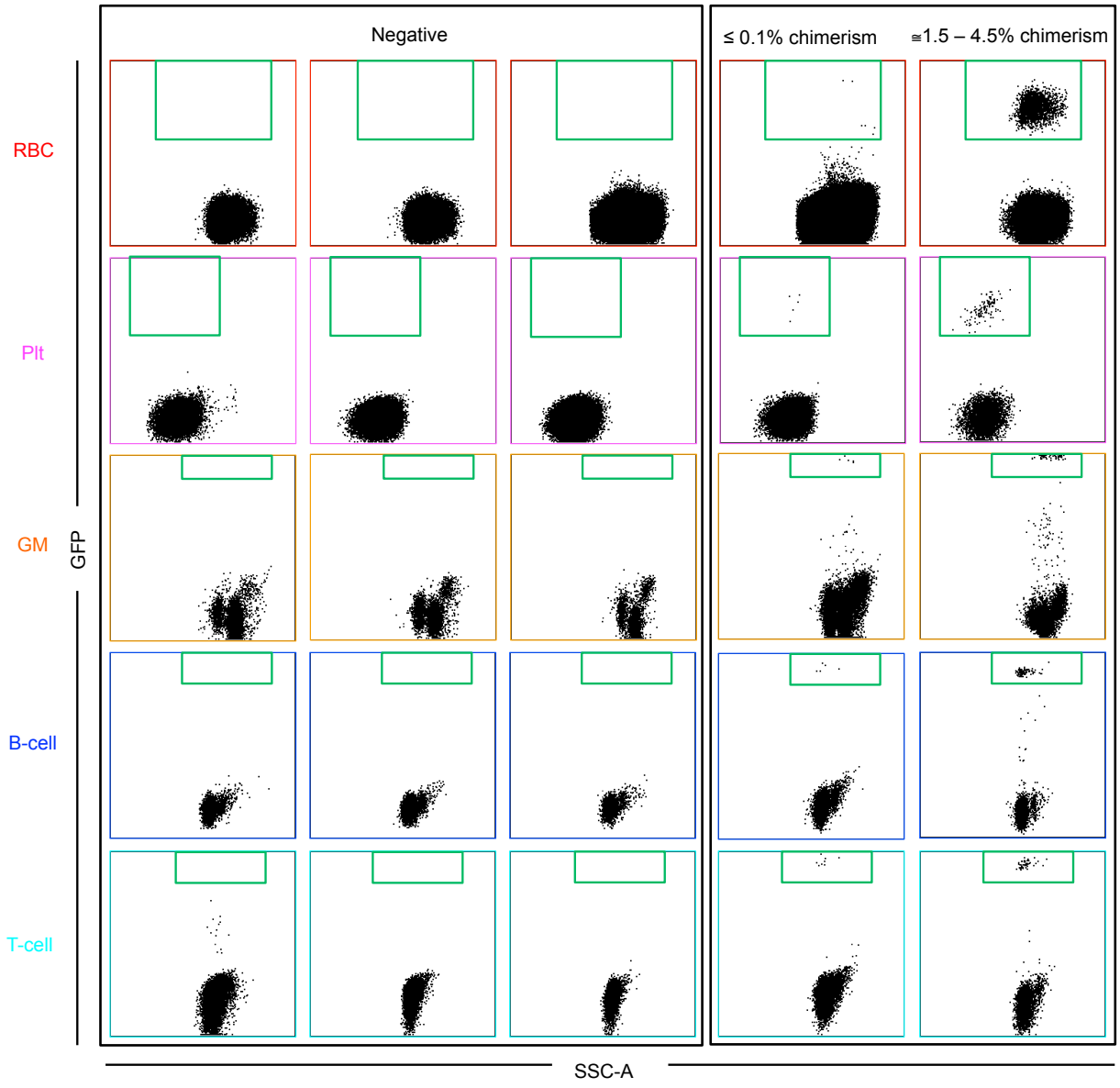

Supplemental Figure 5: Single-cell reconstitution of RBCs, Plts, GM, B, and T cells. Shown are example flow cytometry plots from single-cell transplantation experiments of one UBC-GFP cell into a lethally irradiated wt recipient. The first 3 columns show recipient mice scored as "negative", with no GFP+ cells detected, with RBCs in the top row followed by Plts, GMs, B, and T cells, as indicated. The 4th column show plots from one of the lowest "positive" recipients of each mature cell type, and the 5th (right) column) shows one plot from a robustly reconstituted recipient of each mature cell type. The level of GFP in donor-derived cells of each mature cell type matches that of the level of GFP in unmanipulated donor mice shown in Figure S1C. The use of UBC-GFP donor cells allow for very sensitive detection of donor-derived cells because the GFP signal is very distinct from wt host cells and never detected in untransplanted mice. RBC, red blood cell; Plt, platelet; GM, granulocyte-myelomonocyte.

Supplemental Figure 6

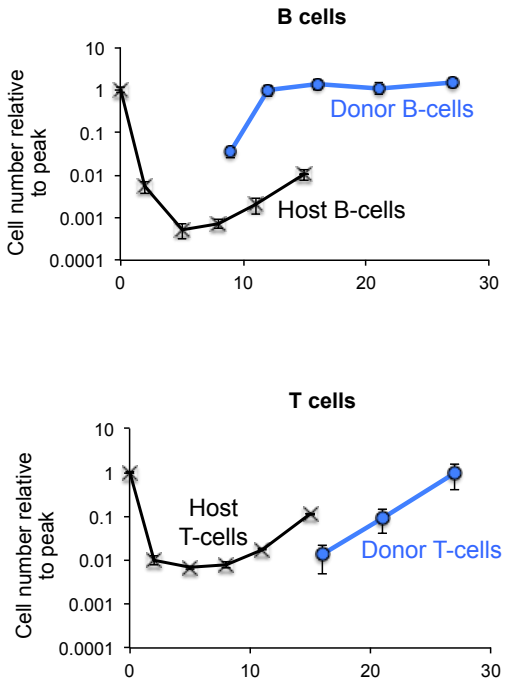

Supplemental Figure 6: CLP^{F}-derived B cells accumulate near the low point of host B cell decline, whereas host T cells recover prior to CLP-derived T cell accumulation. Black lines depict the decline and recovery of host B cells (top) and T cells (bottom) after lethal irradiation. Blue lines indicate donor-derived B cells (top) and T cells (bottom) after transplantation of CLP^{F}.

SUPPLEMENTAL METHODS

Transplantation assays

Hematopoietic cells were isolated from BM isolated from murine femurs and tibias from wild-type (C57Bl6) or UBC-GFP mice (Schaefer et al., 2001) (The Jackson Laboratory, Stock # 004353) in accordance with UCSC guidelines, as described in the supplemental methods and previously (Beaudin et al., 2014, 2016, Smith-Berdan et al., 2011, 2015; Ugarte et al., 2015). Both male and female mice were used as donors and recipients. CD117-enriched bone marrow cells were double-sorted using a FACSAriaIII (BD Biosciences) then transplanted into sublethally (~500 rads) or lethally (~1000 rads) recipients. HSC (Lineage-, cKit+, Sca1+, CD150+, FLK2-), MPP^{F} (Lineage-, cKit+, Sca1+, CD150-, FLK2+), CMP^{-} (Lineage-, $cKit^{+}$, $Sca1^{-}$, $FcγRα^{mid}$, $CD34^{mid}$, $FLK2^{-}$), CMP^{+} (Lineage-, $cKit^{+}$, $Sca1^{-}$, $FcγRα^{mid}$, $CD34^{mid}$, $FLK2^{+}$), MEP (Lineage-, $cKit^{+}$, $Sca1^{-}$, $FcγRα^{lo}$, $CD34^{lo}$), classical GMP (Lineage-, $cKit^{+}$, $Sca1^{-}$, $FcγRα^{hi}$, $CD34^{hi}$), CLP (Lineage-, $cKit^{mid}$, $Sca1^{mid}$, $IL7Rα^{+}$, $FLK2^{+}$), alternative “GMPs” (Lineage-, cKit+, Sca1-, CD41-, FcγRα+), pre-GMs (Lineage-, cKit+, Sca1-, CD41-, FcγRα-, CD105-, CD150-). The lineage cocktail was comprised of CD3 (Biolegend cat #100306), CD4 (Biolegend cat #100423), CD5 (Biolegend cat #100612), CD8 (Biolegend cat #100723), TER-119 (Biolegend cat #116215), Mac1 (Biolegend cat #101217), Gr1 (Biolegend cat #108417), and B220 (Biolegend cat #103225). Antibodies used in sorting were: cKit(Biolegend cat #105826), Sca1 (Biolegend cat #122520), CD150 (Biolegend cat #115914), FLK2 (ebiosciences cat #12-1351-83), CD34 (ebiosciences cat #13-0341-85), IL7Rα (Biolegend cat #135014), CD41 (Biolegend cat #133914), CD105 (Biolegend cat #120402).

Mature cell quantification

A known volume of peripheral blood was mixed with an antibody solution [TER-119 (Biolegend cat #116210), CD61 (Biolegend cat #104314), Mac1 (Biolegend cat #101216), Gr1 (Biolegend cat #108430), B220 (Biolegend cat #103224), CD3 (Biolegend cat #100308)] containing a

known quantity of Calibrite-APC beads (BD Biosciences cat no. 340487) prior to flow cytometry analysis. For tissues, a known quantity of Calibrite-APC beads was added to each tissue preparation prior to antibody staining and analysis. The number of beads counted by flow cytometry for blood and tissue samples was used to calculate the number of mature cells per microliter of blood or within each tissue. RBC (FSC^{lo-mid}, TER-119+, CD61-, Mac1-, Gr1-, B220-, CD3-), Platelets (SSC^{lo}, TER-119-, CD61+, Mac1-, Gr1-, B220-, CD3-), GM (FSC^{mid-hi}, TER-119-, CD61-, Mac1+, Gr1+, B220-, CD3-), B-cell (FSC^{mid}, TER-119-, CD61-, Mac1-, Gr1-, B220+, CD3-), T-cell (FSC^{mid}, TER-119-, CD61-, Mac1-, Gr1-, B220-, CD3+). The distribution of mature hematopoietic cells in a mouse was measured in the blood obtained by perfusion; in bone marrow by analysis of two femurs and tibias; spleen; thymus; and lymph nodes (inguinal, axillary, and superficial cervical).

Single-cell transplants

Individual HSCs and MPP^F were double-sorted into separate wells on Terasaki plates using a FACSAriaIII from lineage-depleted bone marrow cells from UBC-GFP mice, similar to our previous reports (Byrne et al., 2017; Cole et al., 2018). Fluorescence microscopy was used to verify that only one cell occupied each well. Individual cells were loaded into a 0.5 mL syringe pre-loaded with 200,000 WT BM cells. One syringe was used per lethally irradiated (1,000 rads) WT recipient to inject one single HSC or one single MPP^F retroorbitally per recipient. Donor contribution to mature cells was assessed in the peripheral blood weekly from week 2-6 posttransplantation and every other week at later timepoints, as indicated in the x-axis of Figure 4G-J. To ensure high sensitivity, a large number of events (~2.5M) were recorded in low-engrafting recipients. The number of detected donor-derived cells was used to score a recipient as “positive”, rather than an arbitrary chimerism threshold as these percentages are highly influenced by the differential death of host cells (Figure 4O).

CFU-S analysis

Lethally irradiated (1,000 rads) WT mice were transplanted with an equal mixture of double-sorted cells isolated from mT/mG (Muzumdar et al., 2007) and UBC-GFP mice. On day 8.5 (MEP), 9.5 (CMP and CMP^F), 11.5 (MPP^F), and 13.5 (HSC) post-transplantation, mice were sacrificed and perfused to remove peripheral blood. Individual CFU-S were removed with a scalpel under a fluorescent dissecting scope. Single-cell suspensions of dissected colonies were labeled with the following antibodies: TER-119, CD41, Mac1, Gr1, and B220. Cell types were defined as follows: Erythroid Progenitor (EP; FSC^{mid-hi}, TER-119+, CD41-, Mac1-, Gr1-, B220-); Megakaryocyte (Meg; FSC^{mid-hi}, TER-119-, CD41+, Mac1-, Gr1-, B220-); GM (FSC^{mid-hi}, TER-119-, CD41-, Mac1+, Gr1+, B220-); B-cell (FSC^{mid-h},TER-119-, CD41-, Mac1-, Gr1-, B220+).

Analysis and secondary transplantation of HSC- and MPP^F-derived progenitor cells

2.5K HSC or 20K MPP^F were FACS purified from UBC-GFP mice (Schaefer et al., 2001) and transplanted into irradiated WT recipients (C57BL6) (see experimental schematic in Figure 3A) (Beaudin et al., 2014, 2016, Smith-Berdan et al., 2011, 2015; Ugarte et al., 2015). BM was isolated on days 2, 4, 7, 11 and 14 post transplantation and analyzed using the indicated markers. Neither HSCs nor MPP^Fs gave rise to FLK2+ cells due to rapid, irradiation-induced downregulation of FLK2 surface protein on both donor and host cells (manuscript in preparation); thus we utilized CD48 instead of FLK2 to assess presence of substantially overlapping “MPPs” (Pietras et al., 2015). For functional analysis by secondary transplantation, BM was isolated from sternum, hips, femurs and tibias 14 days post transplantation of 2.5K HSC or 20K MPP^F, CD117-enriched, and sorted for GFP+ CMP, GMP, MEP and EP using a FACSAriaIII and the markers as displayed in Fig 3D and F. Donor-derived (GFP+) CMPs (10k cells/mouse), GMPs (50k), MEPs (50k), or EPs (20k) were then transplanted into ¾-lethally irradiated (750 rads) WT recipients (C57BL6) and mature cells from these secondary

transplants were quantified by tail bleeds and flow cytometry analysis as described in the main methods.

Host cell disappearance versus donor-derived cell production

The relative numbers and coincidence of host cell death and donor-derived cell production (Figures 4P-T and S6) were illustrated by plotting the decline in host cell numbers from pre-conditioning, set at **1**, to 30 days post-conditioning, based on data from Figure 1O. Likewise, HSC- or MPP^F-derived donor cells were set to **1** for the peak of cell production based on data from the transplantation experiments of Figure 1-2, with mature cell numbers at other time points within the 30-day period plotted relative to this peak value.

Markov Modeling

To determine if the cells observed in the quantitative plots are a result of generation of new cells or retention of generated cells, over time, we used the Markov Birth-Death Process (Kendall, 1948; Yule, 1925). Experimentally obtained population size, 7 or 9 days post-transplantation, was used as the initial population size for the modeling. Using literature derived half-lives ($T_{1/2}$) for RBCs, Plts, GM, B and T cells as 22, 4.5, 1, 38.5 and 150 days, respectively (Dholakia et al., 2015; Fulcher and Basten, 1997; Nayak et al., 2013; Simon and Kim, 2010; Sprent and Basten, 1973), we determined the death rate probability for each mature cell using the formula:

$$P(D) = Log_e(2) / T_{1/2}$$

Because the population size varies differentially over time, we modified the Markov model to reflect these changes and wrote a Python code to obtain the varying birth rates, and the number of new cells produced between any two time points as depicted in Supplemental Figure 2 (dotted lines) and Supplemental Figure 3C. We also confirmed that the theoretical population size obtained based on the varying birth rates generated by the program was reflective of the

experimental data at the earlier time points, where we measured the cells at “day of peak” (Figure 2A; “burst phase method”).

Python program

The complete code for the Markov birth-death models will be posted on GitHub and freely available to the scientific community upon publication of these results.

Statistical Analysis

Statistical significance was determined by two-tailed unpaired student's T-test, unless otherwise noted. All data are shown as mean ± standard error of the mean (SEM) representing at least two independent experiments.

SUPPLEMENTAL REFERENCES

Beaudin, A.E., Boyer, S.W., and Forsberg, E.C. (2014). Flk2/Flt3 promotes both myeloid and lymphoid development by expanding non-self-renewing multipotent hematopoietic progenitor cells. Exp. Hematol. *42*, 218–229.e4.

Beaudin, A.E., Boyer, S.W., Perez-Cunningham, J., Hernandez, G.E., Derderian, S.C., Jujjavarapu, C., Aaserude, E., MacKenzie, T., and Forsberg, E.C. (2016). A Transient Developmental Hematopoietic Stem Cell Gives Rise to Innate-like B and T Cells. Cell Stem Cell *19*, 768–783.

Dholakia, U., Bandyopadhyay, S., Hod, E.A., and Prestia, K.A. (2015). Determination of RBC survival in C57BL/6 and C57BL/6-Tg(UBC-GFP) mice. Comp. Med.754-61.

Fulcher, D., and Basten, A. (1997). B cell life span: a review. Immunol. Cell Biol.

Kendall, D.G. (1948). On the Generalized “Birth-and-Death” Process. Ann. Math. Stat.

Muzumdar, M.D., Tasic, B., Miyamichi, K., Li, L., and Luo, L. (2007). A global double-fluorescent Cre reporter mouse. Genesis *45*, 593–605.

Nayak, M.K., Kulkarni, P.P., and Dash, D. (2013). Regulatory role of proteasome in determination of platelet life span. J. Biol. Chem. 288(10):6826-34.

Pietras EM, Reynaud D, Kang YA, Carlin D, Calero-Nieto FJ, Leavitt AD, Stuart JM, Göttgens B, Passegué E. (2015). Functionally Distinct Subsets of Lineage-Biased Multipotent Progenitors Control Blood Production in Normal and Regenerative Conditions. Cell Stem Cell.17(1):35-46.

Schaefer, B.C., Schaefer, M.L., Kappler, J.W., Marrack, P., and Kedl, R.M. (2001). Observation of Antigen-Dependent CD8+ T-Cell/ Dendritic Cell Interactions in Vivo. Cell. Immunol. *214*, 110–122.

Simon, S.I., and Kim, M.H. (2010). A day (or 5) in a neutrophil’s life. Blood.

Smith-Berdan, S., Nguyen, A., Hassanein, D., Zimmer, M., Ugarte, F., Ciriza, J., Li, D., García-Ojeda, M.E., Hinck, L., and Forsberg, E.C. (2011). Robo4 cooperates with CXCR4 to specify hematopoietic stem cell localization to bone marrow niches. Cell Stem Cell *8*, 72–83.

Smith-Berdan, S., Nguyen, A., Hong, M.A., and Forsberg, E.C. (2015). ROBO4-mediated vascular integrity regulates the directionality of hematopoietic stem cell trafficking. Stem Cell Reports *4*, 255–268.

Sprent, J., and Basten, A. (1973). Circulating T and B lymphocytes of the mouse. II. Lifespan. Cell. Immunol.

Ugarte, F., Sousae, R., Cinquin, B., Martin, E.W., Krietsch, J., Sanchez, G., Inman, M., Tsang, H., Warr, M., Passegué, E., et al. (2015). Progressive Chromatin Condensation and H3K9 Methylation Regulate the Differentiation of Embryonic and Hematopoietic Stem Cells. Stem Cell Reports *5*, 728–740.

Yule, G.U. (1925). A Mathematical Theory of Evolution, Based on the Conclusions of Dr. J. C.